NMR Studies of Toxin III from the Sea Anemone *Radianthus paumotensis* and Comparison of Its Secondary Structure with Related Toxins†

Joseph H. B. Pease,‡,§ N. Vasant Kumar,‡,§ Hugues Schweitz,∥ Neville R. Kallenbach,⊥ and David E. Wemmer*,‡,§

Department of Chemistry, University of California, and Chemical Biodynamics Division, Lawrence Berkeley Laboratory, 1 Cyclotron Road, Berkeley, California 94720, Centre de Biochimie du CNRS, Faculté des Sciences, Université de Nice, Parc Valrose, 06034 Nice Cedex, France, and Department of Chemistry, New York University, New York, New York 10023

Received August 17, 1988; Revised Manuscript Received October 26, 1988

ABSTRACT: Nearly complete assignments of the proton nuclear magnetic resonance (NMR) spectrum of the polypeptide toxin III from the sea anemone *Radianthus paumotensis* (RP) are presented. The secondary structures of the related toxins RP II and RP III are described and are compared with each other and with another related toxin ATX Ia from *Anemonia sulcata* [Widmer, H., Wagner, G., Schweitz, H., Lazdunski, M., & Wüthrich, K. (1988) *Eur. J. Biochem. 171*, 177–192]. All of these proteins contain a highly twisted four-strand antiparallel β-sheet core connected by loops of irregular structure. From the work done with AP-A from *Anthopleura xanthogrammica* [Gooley, P. R., & Norton, R. S. (1986) *Biochemistry 25*, 2349–2356], it is clear that this homologous toxin also has the same basic core. Some small differences are seen in the structures of these toxins, particularly in the position of the N-terminal residues that form one of the outside strands of the β-sheet. In addition, the *R. paumotensis* toxins are two residues longer, extending the third strand of sheet containing the C-terminal residues. A comparison of chemical shifts for assigned residues is also presented, in general supporting the similarity of structure among these proteins.

Sea anemones produce a variety of small peptide toxins to use as part of their feeding and powerful defense systems (Beress, 1982). These toxins are generally around 50 amino acids in length and have several conserved residues, including all cysteine residues (see Figure 1). Sea anemone toxins are known to bind to Na^+ channels and alter their ion-conducting characteristics by slowing down the inactivation step and hence prolonging the action potential (Romey et al., 1976). Because of their specificity and high affinity for Na^+ channels, these toxins have been used as tools in the study of excitable membranes (Rathmayer, 1979). Determination of structures for these toxins would help to further characterize conformational features required for binding to the Na^+ channels. Recently, resonance assignments and the secondary structures of several sea anemone toxins have been determined by using two-dimensional nuclear magnetic resonance spectroscopy (2D-NMR).[1] Gooley and Norton studied toxin I from *Anemonia sulcata* (ATX I) (Gooley et al., 1984; Gooley & Norton, 1986b) and anthopleurin A from *Anthopleura xanthogrammica* (AP-A) (Gooley & Norton, 1985, 1986a). More recently, Widmer and co-workers further purified ATX I and obtained complete proton NMR assignments for ATX Ia (Widmer et al., 1988). Our laboratory, on the other hand, is studying the structures of toxin II (RP II) (Wemmer et al., 1986) and toxin III (RP III) from the sea anemone *Radianthus paumotensis*.

The purification and the immunological and pharmacological properties of the toxins from *R. paumotensis* have been discussed previously (Schweitz et al., 1985). It was found that toxins from *R. paumotensis* form a distinct immunological class, even though they have significant sequence homology with the toxins from *A. sulcata* and *A. xanthogrammica* (Figure 1). Antibodies to RP III recognize the other *R. paumotensis* toxins but not toxins from *A. sulcata* or *A. xanthogrammica*, and conversely antibodies against toxins from *A. sulcata* (ATX II and ATX V) and *A. xanthogrammica* (AP-A and AP-B) do not recognize the *R. paumotensis* toxins. It is also interesting that toxins from *R. paumotensis* do not affect the binding of the toxins from *A. sulcata* to the Na^+ channels. Instead the *R. paumotensis* toxins compete with a toxin from the scorpion *Androctonus australis* (toxin AA II) for binding sites on the Na^+ channels even though AA II has no sequence homology with the *R. paumotensis* toxins (it is longer, 64 vs 48 residues, and contains four disulfides instead of three; Rochat et al., 1972). It is hoped the determination of the structures of these toxins will lead to a better understanding of this behavior.

Our laboratory recently reported the assignment of RP II's proton NMR spectrum (Wemmer et al., 1986). The sequential assignment pattern and the observation of certain kinds of long-range NOEs (between residues far apart in sequence; Wüthrich et al., 1984) led to the determination of RP II's secondary structure. This structure contains a core of antiparallel β-sheet connected by loops of irregular structure, with no helical content. The reported secondary structures of toxins from other sea anemones also contain the same general pattern (Gooley & Norton, 1986a; Widmer et al., 1988). In this work we describe the assignments and compare

† This work was supported by the Office of Energy Research, Office of Health and Environmental Research, Health Effects Research Division of the U.S. Department of Energy, under Contract No. DE-AC03-76SF00098 (D.E.W.), by National Institutes of Health Grant GM 31861 (N.R.K.), and through instrumentation grants from the U.S. Department of Energy, DE FG05-86ER75281, and the National Science Foundation, DMB 86-09035 (D.E.W.).

‡ University of California.
§ Lawrence Berkeley Laboratory.
∥ Université de Nice.
⊥ New York University.

[1] Abbreviations: 2D, two-dimensional; NMR, nuclear magnetic resonance; COSY, 2D correlated spectroscopy; RELAY, 2D relayed coherence transfer spectroscopy; NOESY, 2D nuclear Overhauser effect spectroscopy; NOE, nuclear Overhauser effect; ATX I, toxin I from *Anemonia sulcata*; AP-A, anthopleurin A from *Anthopleura xanthogrammica*; RM III, toxin III from *Radianthus macrodactylus*; RP II and RP III, toxin II and toxin III from *Radianthus paumotensis*.

0006-2960/89/0428-2199$01.50/0

Radianthus paumotensis II (RP II)	-ASCKCDDDGPDVRSATFTGTVDFWN--CNEGWEKCTAVYTPVASCCRKKK
Radianthus paumotensis III (RP III)	-GNCKCDDEGPNVRTAPLTGYVDLGY--CNEGWEKCASYYSPIAECCRKKK
Stichodactyla helianthus I (SH I)	-AACKCDDEGPDIRTAPLTGTVDLGS--CNAGWEKCASYYTIIADCCRKKK
Anemonia sulcata Ia (ATX Ia)	GAACLCKSDGPNTRGNSMSGTIWVF--GCPSGWNNCEGRA-IIGYCCKQ
Anemonia sulcata II (ATX II)	GVPCLCDSDGPSVRGNTLSGIIWLA--GCPSGWHNCKKHGPTIGWCCKQ
Anthopleura xanthogrammica (AP-A)	GVSCLCDSDGPSVRGNTLSGTLWLYPSGCPSGWHNCKAHGPTIGWCCKQ

FIGURE 1: Sequences of sea anemone toxins. Other known variants include *Radianthus macrodactylus* III (RM III; differs from RP III in N → Y at position 11); *A. sulcata* Ib (ATX Ib; differs from ATX Ia in A → P at position 3); *A. sulcata* V (ATX V; differs from ATX II in G → K at position 37 and deletion of the C-terminal Q); *A. xanthogrammica* B (AP-B; differs from A in S → P at position 3; SV → RP at positions 11 and 12; T → I at position 20; L → F at position 23; T → N at position 39; and Q → K at position 46). References: RP II (Wemmer et al., 1986), RP III (Metrione et al., 1988), SH I (Kem, 1987), ATX Ia and ATX Ib (Wunderer & Eulitz, 1978), ATX II (Wunderer et al., 1976), AP-A (Tanaka et al., 1977), RM III (Zykova et al., 1986), ATX V (Scheffler et al., 1982), AP-B (Reimer et al., 1985).

in some detail the secondary structure of RP III with these toxins.

Materials and Methods

NMR Spectroscopy. The purification (Schweitz et al., 1985) and primary sequence (Metrione et al., 1987) of RP III have been described previously. A sample containing ca. 14 mg of peptide was dissolved in 400 μL of either D_2O or 90% H_2O/10% D_2O at pH 4.6. All two-dimensional spectra were recorded on either a General Electric GN-500 or a Bruker AM-500 spectrometer operating at 500-MHz ^1H frequency. COSY (Wider et al., 1984), RELAY (Eich et al., 1982; Bax & Drobny, 1985), and NOESY (Wider et al., 1984) spectra were recorded at temperatures between 10 and 37 °C to obtain sequential assignments. Different temperatures were used to shift the water resonance relative to the protein resonances so that α-proton resonances close to the water peak could be observed. Some chemical shifts in the protein change slightly with temperature, aiding assignments of near degenerate proton frequencies. All COSY spectra were recorded in magnitude mode except for one phase-sensitive double-quantum filtered COSY spectrum in D_2O. All RELAY spectra were done in magnitude mode with total mixing delays between 25 and 40 ms. Phase-sensitive NOESY spectra were used with mixing times from 200 to 300 ms. Phase-sensitive spectra were obtained by using time proportional phase incrementation (TPPI) (Drobny et al., 1979). Each spectrum had 512 t_1 points and 1024 complex t_2 data points. Data were zero filled in the t_1 dimension to yield final 1024 × 1024 point real matrices. Spectral widths of 5952 Hz (6 Hz/point) and 5000 Hz (5 Hz/point) were used for H_2O and D_2O spectra, respectively. Suppression of the residual water peak was achieved by using continuous low-power irradiation during the relaxation delay and the mixing time (NOESY). Sine bell apodization with 0° phase shift was used in both dimensions of the magnitude COSY and RELAY spectra. A skewed sine bell apodization (Hare et al., 1985) was used in both dimensions with a skew of 0.6 and a phase shift of 30° for NOESY spectra and 10° for the double-quantum filtered COSY spectrum. The first row of the (t_1, ω_2) matrix was multiplied by 0.5 before the t_1 transform to suppress t_1 ridges (Otting et al., 1986). All data processing was done by using FTNMR program (D. Hare, unpublished data) on either a Micro Vax II or a Vax 11/785.

Results and Discussion

The assignment of RP III's ^1H NMR spectrum was carried out by using the sequential approach developed by Wüthrich and co-workers (Wüthrich et al., 1982; Billeter et al., 1982; Wüthrich, 1983). Since this process has been described in detail in the literature for general cases, and specifically for RP II (Wemmer et al., 1986), we will not repeat the details of the assignment process here. There were no unusual problems associated with determining the assignments, and the only question remaining concerns the reported sequence (Metrione et al., 1987). The presence of a third lysine at the C terminus was ambiguous in the chemical sequencing of both RP II and RP III, but the NMR data indicate that an extra residue (with a long side chain) is clearly present in this position. While the NMR cannot distinguish between lysine and arginine in this case, from the compositions reported (Schweitz et al., 1985) it is almost certainly lysine. A summary of the observed sequential connectivities is given in Figure 2, and the chemical shifts of all assigned protons are listed in Table I. Some of the long side chain proton resonances were unassignable due to the chemical shift degeneracy of many of these protons. The fingerprint region, with labeled amide to α-proton intraresidue COSY cross peaks, is shown in Figure 3.

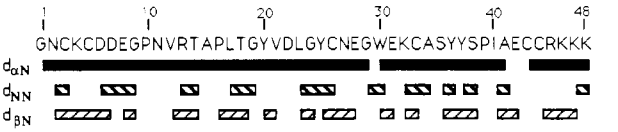

FIGURE 2: Summary of the sequential NOEs observed for RP III. A bar connecting residues indicates the connectivity was observed. For the residues preceding a Pro, the $d_{\alpha N}$ connectivity means the NOE between the α-proton of the previous residue to the Pro δ-protons was observed.

The dominant sequential connectivity is of the $d_{\alpha N}$ type, showing that the majority of residues are in an extended conformation, such as that found in regions of β-sheet (Wüthrich et al., 1984). There are only a few scattered NOEs of the d_{NN} type with no stretches of more than four consecutive residues; therefore, the peptide has no regular helix. The observed α-proton to α-proton NOEs, in Figure 4, indicate the presence of the four-stranded antiparallel β-sheet structure shown in Figure 5. This sheet structure is further confirmed by the presence of several other long-range NOEs and by the presence of hydrogen bonds deduced from slow amide exchange. Slowly exchanging amides were determined by first lyophilizing the sample from H_2O, then redissolving it in D_2O, and immediately running a COSY experiment, shown in Figure 6. Amide to α-proton cross peaks present in this spectrum indicate those amide protons most protected against exchange with solvent, presumably through hydrogen bonding. These include residues 20–22, 30, 31, 33, and 41–45 for RP III. The cysteine pairing to form the disulfides (Cys-3 with 43, Cys-5 with 33, and Cys-26 with 44) forces the β-sheet core to be highly twisted. The disulfides are presumed to be in the

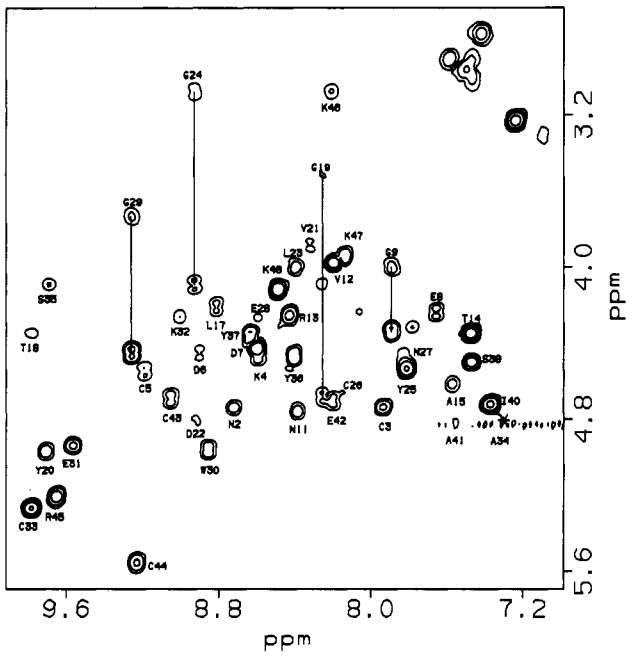

FIGURE 3: Fingerprint region of the COSY spectrum of RP III in H_2O at 20 °C. Cross peaks correspond to intraresidue amide-proton to α-proton connectivities. Cross peaks are labeled with the standard one-letter code. Unlabeled cross peaks in the top right-hand corner of the spectrum are from side-chain protons. The lines connect the two cross peaks associated with each glycine α-proton resonance.

same location as in AP-A (Norton, 1981) and toxin II from *A. sulcata* (Wunderer, 1978) due to the conservation of cysteine residues and the similarity of secondary structure among these toxins. The NOE connectivity patterns in the loops connecting the β-sheet strands, comprised of residues 6–16, 24–27, and 34–42, show that there are no other regions of regular secondary structure, except for a type II β-turn involving residues 27–30. This turn is clearly indicated by the slow exchange of Trp-30's amide (hydrogen bonding to Asn-27's backbone carbonyl) and the NOE intensity pattern: $d_{\alpha N}$ (28–29) is strong, d_{NN} (29–30) is strong, and $d_{\alpha N}$ (28–30) is weak (Wüthrich et al., 1984). The basic structural pattern of the β-sheet core and type II β-turn is present in all the other anemone toxins studied thus far: RP II, AP-A (Gooley & Norton, 1986a), and ATX Ia (Widmer et al., 1988).

In comparing the secondary structures of these proteins we do find some differences in structure. The αH(2) to αH(20) NOESY cross peak is much weaker for RP III than for RP II, while the αH(4) to αH(17) cross peak is very weak in RP II but is quite strong in RP III (it was identified in RP II only after its clear presence in RP III was noted). These two NOESY cross peaks in combination with an NH to NH NOE between residues 18 and 19 indicate the presence of a β-bulge in both RP II and RP III (Figure 5). This region of ATX Ia also contains a β-bulge, but with the two αH–αH NOE peaks apparently of normal intensity (Widmer et al., 1988). The differences in NOE intensities in this region between RP II and RP III indicate that the N-terminal strand of the β-sheet in RP III is translated quite significantly (the order of 1.5 Å) relative to its neighboring strand. This strand in ATX Ia is probably translated to a lesser extent than in RP III. The region containing this β-bulge is quite interesting. The Gly residue at position 19 is one of very few non-cysteine residues that is completely conserved among the anemone toxins (Figure 1). This suggests that the unusual structure formed is functionally important in the protein and requires glycine at this position, probably to prevent a clash between the side chain of this residue and the neighboring strand of β-sheet. This β-bulge does not fit any of the categories described by Richardson (1981). The residue preceding this Gly is always Thr or Ser; however, a variety of residues are observed following it. Interactions of the hydrophobic side chain of residue 17 (Leu, Phe, or Met) may play a role in determining the conformation of the loop containing residues 6–16. In RP II the aromatic ring protons of the Phe-17 are close to the methyls of Val-12, but in RP III no cross peaks are seen between the methyls of Leu-17 and those of Val-12. In both peptides clear contacts between several of the aromatic and methyl-containing residues are present and very similar in intensity, showing that the overall tertiary structure is in fact quite similar. Once the complete three-dimensional structures of these proteins have been determined by distance geometry calculations (presently under way), the basis for the differences in long-range NOEs will be more clearly understood.

Table I: Chemical Shifts of Assigned Resonances, pH 4.6, 20 °C[a]

residue	amide	α-H	β-H	other
Gly-1	*b*	3.49, 2.54		
Asn-2	8.78	4.70	3.00, 2.64	
Cys-3	7.98	4.72	2.88, 2.77	
Lys-4	8.65	4.47	1.81, 1.76	γ 1.47, 1.44
Cys-5	9.25	4.54	3.21, 2.69	
Asp-6	8.96	4.41	2.86, 2.71	
Asp-7	8.66	4.37	2.99, 2.60	
Glu-8	7.70	4.19	2.30, 1.97	γ 2.36, 2.33
Gly-9	7.94	4.34, 3.96		
Pro-10		4.40	2.22, 1.96	γ 2.02, 1.94; δ 3.69, 3.55
Asn-11	8.44	4.74	2.95, 2.68	
Val-12	8.24	3.93	2.15	CH_3 0.96, 0.95
Arg-13	8.48	4.23	1.88, 1.88	
Thr-14	7.51	4.34	4.38	CH_3 1.08
Ala-15	7.61	4.60	1.47	
Pro-16		4.28	2.22, 1.77	γ 2.00, 190; δ 3.92, 3.78
Leu-17	8.87	4.16	2.04, 0.69	γ 1.48; CH_3 0.68, 0.62
Thr-18	9.86	4.34	4.31	CH_3 1.15
Tyr-20	9.78	4.95	2.55, 2.55	δ 7.33; ϵ 6.90
Val-21	8.37	3.88	1.57	CH_3 0.42, 0.24
Asp-22	8.98	4.79	2.55, 2.55	
Leu-23	8.45	3.98	1.54, 1.47	γ 1.49; CH_3 0.86, 0.79
Gly-24	8.99	4.07, 3.03		
Tyr-25	7.86	4.52	3.10, 2.74	δ 7.10; ϵ 6.81
Cys-26	8.20	4.67	2.91, 2.55	
Asn-27	7.87	4.44	2.70, 1.94	
Glu-28	8.65	4.24	2.39, 2.09	
Gly-29	9.32	4.44, 3.71		
Trp-30	8.92	4.94	3.56, 2.93	δ 7.25; ϵ_3 7.06; ζ_2 7.36; ζ_3 7.36; η 6.77; HN 10.45
Glu-31	9.64	4.92	2.03, 1.87	γ 2.22, 2.11
Lys-32	9.07	4.24	1.69, 1.64	
Cys-33	9.86	5.24	3.28, 3.00	
Ala-34	7.34	4.81	1.48	
Ser-35	9.76	4.07	3.96, 3.96	
Tyr-36	8.46	4.46	3.01, 2.64	δ 7.04; ϵ 6.63
Tyr-37	8.69	4.34	2.88, 2.78	δ 7.09; ϵ 6.68
Ser-38	7.51	4.49	4.05, 3.30	
Pro-39		4.63	2.59, 1.93	γ 2.08, 2.08; δ 3.96, 3.68
Ile-40	7.41	4.71	2.15	γ 1.05, 0.90; CH_3 β 0.85; γ 0.80
Ala-41	7.60	4.78	1.19	
Glu-42	8.25	4.73	1.92, 1.40	γ 2.54, 2.24
Cys-43	9.11	4.67	2.78, 2.31	
Cys-44	9.30	5.54	3.00, 3.00	
Arg-45	9.73	5.18	1.91, 1.82	
Lys-46	8.26	3.04	1.11, 0.37	γ 0.55, 0.25; δ 1.12; ϵ 2.76, 2.76; HN_3 7.46
Lys-47	8.19	3.91	1.69, 1.40	γ 1.28, 1.10; δ 1.54, 1.49; ϵ 2.88, 2.88
Lys-48	8.54	4.08	1.71, 1.71	γ 1.35, 1.29

[a] Chemical shifts are in ppm (parts per million) indirectly referenced to TSP [sodium (trimethylsilyl)propionate] by using the water peak at 4.85 ppm. [b] Resonance that could not be assigned in the spectrum.

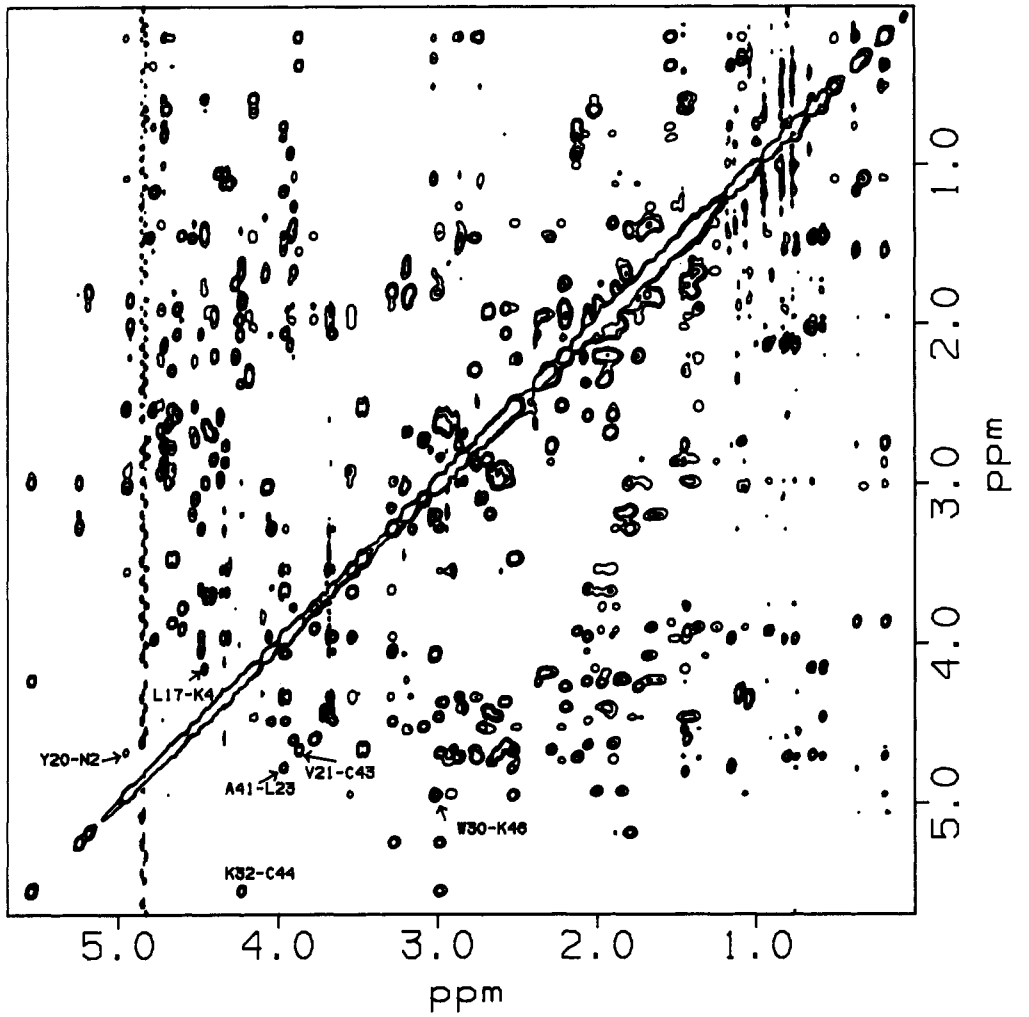

FIGURE 4: Upfield region of a 20 °C NOESY spectrum of RP III in D_2O. A mixing time of 250 ms was used. Interstrand α-proton to α-proton NOE peaks in the β-sheet core are labeled with the standard one-letter code.

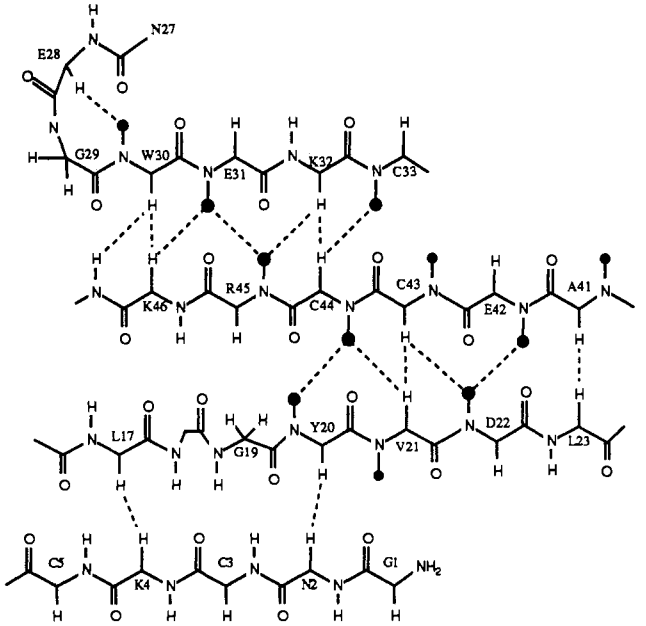

FIGURE 5: Secondary structure of RP III. Dashed lines indicate long-range NOE connectivities, and filled circles represent the slowly exchanging amide protons.

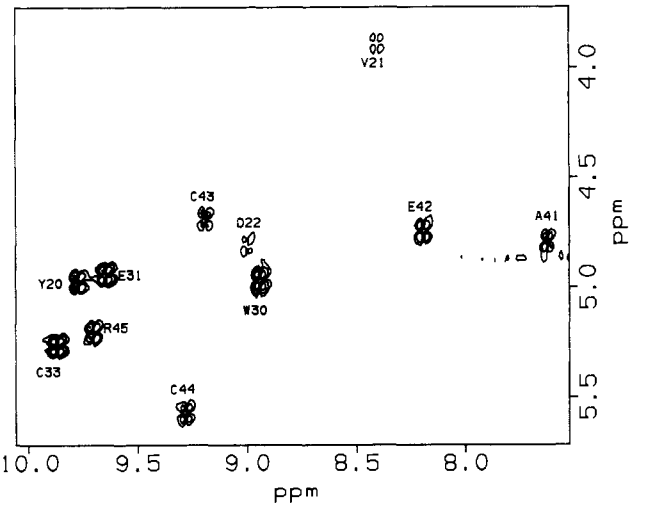

FIGURE 6: Fingerprint region of the double-quantum filtered COSY spectrum of RP III in D_2O at 20 °C. Cross peaks correspond to slowly exchanging amide to α-proton connectivities, which are labeled with the standard one-letter code.

We have compared the chemical shifts of RP II, RP III, and ATX Ia and find strong similarities, for residues both within the β-sheet core and in loops. This is hardly surprising for RP II vs RP III since 31 of 48 amino acids are identical; however, it is also true for RP III vs ATX Ia even though only 14 residues match. This is diagrammed schematically in Figure 7, in which the deviations in chemical shift from the random coil value are shown (Bundi & Wüthrich, 1979). There are a number of differences in aromatic residues among

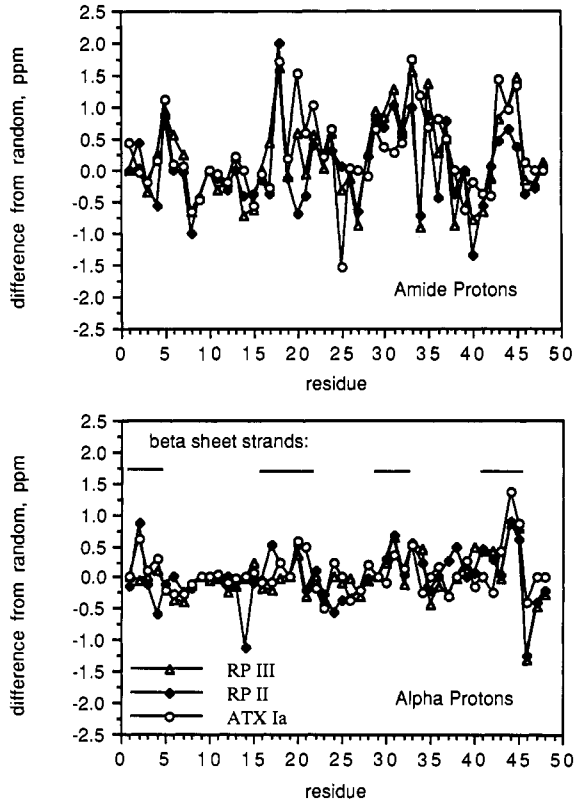

FIGURE 7: Plots of deviations of chemical shifts ($\Delta\delta$) from random coil ($\Delta\delta = \delta_{protein} - \delta_{random\ coil}$) values for RP II (Wemmer et al., 1986), RP III, and ATX Ia (Widmer et al., 1988) as a function of position in the sequence. Plots are shown for amide protons (top) and α-protons (bottom). $\delta_{random\ coil}$ is from Bundi and Wüthrich (1979).

the three toxins RP II, RP III, and ATX Ia. Some of the differences in chemical shift are attributable to ring currents, even though coordinates for the structure are not yet accurately known. Residue 17 is Phe in RP II, but Leu in RP III and Met in ATX Ia. NOEs observed between the side chain of Phe-17 and residues 4 and 14 suggest that ring currents are responsible for the upfield shifts of the αH resonances of these two amino acid residues (Figure 7); chemical shifts are normal for the other two proteins. The residues between 22 and 25 have several changes in aromatics, which must contribute to the spread of both αH and NH chemical shifts for amino acids in this region. Similarly, changes in residues near 36 and 37 may stem from changes in tyrosines: RP III YY → RP II VY → ATX Ia RA. The dramatic shifts (both upfield and downfield) of residues near the C terminus (44–46) in all of the proteins stem from ring currents arising from the conserved Trp at position 30. This is demonstrated both from the secondary structure (Figure 5) and through NOEs involving this aromatic side chain and residue 45.

In the case of inhibitors (of known structure) studied by Pardi et al. (1983), it was clear that conserved structural features often gave rise to similar chemical shifts, although the basis for shifts away from random coil values are uncertain. It is interesting to note the strong similarity in chemical shifts for residues 6–17 for all of the proteins discussed here. In this region the deviations from random coil values are all quite small, probably reflecting the lack of regular secondary structure. This suggests (though it certainly does not prove) that the structure (or lack thereof) of the 6–17 loop is really quite similar in these proteins. This is of interest since sequential connectivities show it to be irregular in secondary structure, but it contains several residues implicated as important in toxicity. Residues Asp-8 and Arg-13 (RP II sequence) that have been found to be important for activity in other anemone toxins (Barhanin et al., 1981) are found in this loop. Arg-13 is the only completely conserved residue known to be involved in binding of toxin to its receptor. RP III and RM III from *Radianthus macrodactylus* have a Glu at position 8 instead of an Asp like all of the other toxins. This substitution may explain RP III's greater toxicity than RP II (Schweitz et al., 1985).

We have presented the resonance assignments for toxin III from the anemone *R. paumotensis*. From the pattern of sequential connectivities, slowly exchanging amide protons, and αH–αH NOEs, it is clear that its secondary structure is very similar to that of previously studied toxins RP II and ATX Ia, including a twisted four-stranded β-sheet and a type II β-turn connected by loops of irregular secondary structure. The position of Rp III's outside strand of the sheet involving residues 1–5, with respect to the neighboring strand, appears to be intermediate between ATX Ia and RP II even though the primary sequences of RP III and ATX Ia are less similar than those of RP II and RP III. Distance geometry calculations are being carried out to determine the three-dimensional structures of ATX Ia (Widmer et al., 1988) and the two RP toxins (our laboratory). A crystal structure of AP-A is also being determined (Smith et al., 1984). Together these structures will lead to a better understanding of the differences between the toxins and give some insight into their mode of action on Na^+ channels.

REFERENCES

Barhanin, J., Hugues, M., Schweitz, H., Vincent, J. P., & Lazdunski, M. (1981) *J. Biol. Chem. 256*, 5764–5769.

Bax, A., & Drobny, G. (1985) *J. Magn. Reson. 61*, 306–320.

Beress, L. (1982) *Pure Appl. Chem. 54*, 1981–1994.

Billeter, M., Braun, W., & Wüthrich, K. (1982) *J. Mol. Biol. 155*, 321–346.

Bundi, A., & Wüthrich, K. (1979) *Biopolymers 18*, 285–298.

Drobny, G., Pines, A., Sinton, S., Weitekamp, D., & Wemmer, D. (1979) *Faraday Div. Chem. Soc. Symp. 13*, 49–55.

Eich, G., Bodenhausen, G., & Ernst, R. R. (1982) *J. Am. Chem. Soc. 104*, 3731–3732.

Gooley, P. R., & Norton, R. S. (1984) *Biochemistry 23*, 2144–2152.

Gooley, P. R., & Norton, R. S. (1985) *Eur. J. Biochem. 153*, 529–539.

Gooley, P. R., & Norton, R. S. (1986a) *Biochemistry 25*, 2349–2356.

Gooley, P. R., & Norton, R. S. (1986b) *Biopolymers 25*, 489–506.

Hare, D. R., Ribeiro, N. S., Wemmer, D. E., & Reid, B. R. (1985) *Biochemistry 24*, 4300–4306.

Kem, W. R. (1987) presented at the Natural Toxins from Aquatic and Marine Environments Meeting at Woods Hole, MA.

Metrione, R. M., Schweitz, H., & Walsh, K. A. (1987) *FEBS Lett. 218*, 59–62.

Norton, T. R. (1981) *Fed. Proc. 40*, 21–25.

Otting, G., Widmer, H., Wagner, G., & Wüthrich, K. (1986) *J. Magn. Reson. 66*, 187–193.

Pardi, A., Wagner, G., & Wüthrich, K. (1983) *Eur. J. Biochem. 137*, 445–454.

Rathmayer, W. (1979) *Adv. Cytopharmacol. 3*, 335–344.

Reimer, N. S., Yasunobu, C. L., Yasunobu, K. T., & Norton, T. R. (1985) *J. Biol. Chem. 260*, 8690–8693.

Richardson, J. S. (1981) *Adv. Protein Chem. 34*, 167–339.

Rochat, H., Rochat, C., Sampieri, F., & Miranda, F. (1972) *Eur. J. Biochem. 28*, 381–388.

Romey, G., Abita, J. P., Schweitz, H., Wunderer, G., & Lazdunski, M. (1976) *Proc. Natl. Acad. Sci. U.S.A. 73*, 4055–4059.
Scheffler, J.-J., Tsugita, A., Linden, G., Schweitz, H., & Lazdunski, M. (1982) *Biochem. Biophys. Res. Commun. 107*, 272–278.
Schweitz, H., Bidard, J.-N., Frelin, C., Pauron, D., Vijverberg, H. P. M., Mahassneh, D. M., & Lazdunski, M. (1985) *Biochemistry 24*, 3554–3561.
Smith, C. D., DeLucas, L., Ealick, S. E., Schweitz, H., Lazdunski, M., & Bugg, C. E. (1984) *J. Biol. Chem. 259*, 8010–8011.
Tanaka, M., Haniu, M., Yasunobu, K. T., & Norton, T. R. (1977) *Biochemistry 16*, 204–208.
Wemmer, D. E., Kumar, N. V., Metrione, R. M., Lazdunski, M., Drobny, G., & Kallenbach, N. R. (1986) *Biochemistry 25*, 6842–6849.
Wider, G., Macura, S., Kumar, A., Ernst, R. R., & Wüthrich, K. (1984) *J. Magn. Reson. 56*, 207–234.
Widmer, H., Wagner, G., Schweitz, H., Lazdunski, M., & Wüthrich, K. (1988) *Eur. J. Biochem. 171*, 177–192.
Wunderer, G. (1978) *Hoppe-Seyler's Z. Physiol. Chem. 359*, 1193–1201.
Wunderer, G., & Eulitz, M. (1978) *Eur. J. Biochem. 89*, 11–17.
Wunderer, G., Fritz, H., Wachter, E., & Machleidt, W. (1976) *Eur. J. Biochem. 68*, 193–198.
Wüthrich, K. (1983) *Biopolymers 22*, 131–138.
Wüthrich, K., Wider, G., Wagner, G., & Braun, W. (1982) *J. Mol. Biol. 155*, 311–319.
Wüthrich, K., Billeter, M., & Braun, W. (1984) *J. Mol. Biol. 180*, 715–740.
Zykova, T. A., Vinokurov, L. M., Kozlovskaya, E. P., & Elyakov, G. B. (1986) *Bioorg. Khim. 11*, 159–165.

Fluorescent Modification and Orientation of Myosin Sulfhydryl 2 in Skeletal Muscle Fibers†

Katalin Ajtai‡ and Thomas P. Burghardt*,§
Department of Biochemistry and Molecular Biology, Mayo Foundation, Rochester, Minnesota 55905
Received July 29, 1988; Revised Manuscript Received October 18, 1988

ABSTRACT: We describe a protocol for the selective covalent labeling of the sulfhydryl 2 (SH2) on the myosin cross-bridge in glycerinated muscle fibers using the sulfhydryl-selective label 4-[*N*-[(iodoacetoxy)ethyl]-*N*-methylamino]-7-nitrobenz-2-oxa-1,3-diazole (IANBD). The protocol promotes the specificity of IANBD by using the ability to protect sulfhydryl 1 (SH1) from modification by binding the cross-bridge to the actin filament and using cross-bridge-bound MgADP to promote the accessibility of SH2. We determined the specificity of the probe using fluorescence gel scanning of fiber-extracted proteins to isolate the probe on myosin subfragment 1 (S1), limited proteolysis of the purified S1 to isolate the probe on the 20-kilodalton fragment of S1, and titration of the free SH1's on purified S1 using the radiolabeled SH1-specific reagent [^{14}C]iodoacetamide or enzymatic activity measurements. We estimated the distribution of the IANBD on the fiber proteins to be ~77% on SH2, ~5% on SH1, and ~18% on troponin I. We characterized the angular distribution of the IANBD on cross-bridges in fibers when the fibers are in rigor, in relaxation, in the presence of MgADP, and in isometric contraction using wavelength-dependent fluorescence polarization [Ajtai, K., & Burghardt, T. P. (1987) *Biochemistry 26*, 4517–4523]. With wavelength-dependent fluorescence polarization we use the ability to rotate the transition dipole in the molecular frame using excitation wavelength variation to investigate the three angular degrees of freedom of the cross-bridge. We find that the SH2 probe distinguishes the different states of the fiber such that rigor and MgADP are ordered and maintain a similar orientation throughout the excitation wavelength domain. The relaxed cross-bridge is ordered and has an orientation that is distinct from the orientation of the cross-bridge in rigor and MgADP over the entire wavelength domain. The active isometric cross-bridge is also ordered and has a distinctive polarization spectrum that has a different shape from all of the other states measured. The active isometric cross-bridge is also oriented differently from the other states, suggesting the presence of a predominant actin-bound cross-bridge state that precedes the power stroke during muscle contraction.

Motions of protein elements of the contractile apparatus in skeletal muscle are often studied by the specific modification of reactive side chains on the protein elements. The fast-reacting thiol, sulfhydryl 1 (SH1), of the myosin cross-bridge was specifically modified by a variety of fluorescent and electron spin resonance (ESR) probes and its orientation studied for many years (Nihei et al., 1974; Borejdo & Putnam, 1977; Thomas & Cooke, 1980; Borejo et al., 1982; Ajtai & Burghardt, 1986). Although the conclusion remains somewhat controversial, it is generally accepted that when myosin is bound to actin the SH1 thiol maintains more than one orientation relative to the actin filament in a muscle fiber. The angular disposition of other points on the myosin cross-bridge was less thoroughly studied, but there is some noteworthy data. The nucleotide binding site on the myosin cross-bridge was noncovalently probed with fluorescent (Yanagida, 1981, 1985) and spin analogues (Crowder & Cooke, 1987). These studies

† This work was supported by a grant from the Mayo Foundation.
‡ On leave from the Department of Biochemistry, Eötvös Loránd University, Budapest, Hungary.
§ Established Investigator of the American Heart Association.

0006-2960/89/0428-2204$01.50/0